Stability of spiral wave vortex filaments with phase twists

Keeyeol Nam,* Edward Ott,† Parvez N. Guzdar, and Michael Gabbay‡
Institute for Plasma Research, University of Maryland, College Park, Maryland 20742
(Received 24 February 1998)

In this paper we investigate the stability of a straight vortex filament with phase twist described by the three-dimensional complex Ginzburg-Landau equation (CGLE). The results of the linear stability analysis show that the straight filament is stable in a limited region of the two parameter space of the CGLE. The stable region is dependent on the phase twist imposed on the filament and shrinks in size as the phase twist is increased. It is also shown numerically that the nonlinear evolution of an unstable initial straight filament can lead to a helical filament. [S1063-651X(98)13508-0]

PACS number(s): 82.40.Ck, 47.20.−k, 47.54.+r, 47.32.Cc

I. INTRODUCTION

Pattern formation in nonequilibrium systems has been a very active area of research in recent years [1,2]. Diffusing reacting chemicals, colonies of social amoebae, and propagation of electrical excitations in the heart are typical examples of such systems [1]. One of the simplest mathematical equations which has been investigated extensively for pattern formation is the complex Ginzburg-Landau equation (CGLE),

$$\frac{\partial A}{\partial t} = A - (1+i\alpha)|A|^2 A + (1+i\beta)\nabla^2 A, \tag{1}$$

where A is the complex order parameter which governs the slow spatial and temporal behavior of the system, and α and β are real numbers. This equation can be derived when the homogeneous state of a spatially extended system is in the vicinity of a Hopf bifurcation [1,2]. Although the CGLE is strictly only valid near the bifurcation, it often shows qualitative behavior very similar to physical systems even in parameter regimes far from the bifurcation point. One- and two-dimensional analyses of the CGLE have been the subject of exhaustive studies over the last two decades. For example, the dynamics of the spiral wave solution [3], spiral wave domain patterns [4], and the transition to spatiotemporal chaos [5–8] in two dimensions have been extensively investigated. However, study of the three-dimensional (3D) CGLE has received attention only recently. Using perturbation theory, the evolution of scroll wave filaments (the three-dimensional analog of the 2D spiral waves) has been investigated in the regime where straight filaments are stable [9]. For example, in the special case of a circular filament with radius R, the rate of collapse of the ring is governed by the equation $dR/dt = -(1+\beta^2)/R$. For the parameter region where β is larger than $\beta_c(\alpha)$ it was shown in Ref. [10] that a straight vortex filament becomes unstable to perturbations along its length. They also see stable evolution of the instability to apparently stable helices. In the analytical part of their work the authors of Ref. [10] have derived this instability as a three-dimensional extension of the two-dimensional core instability of spiral waves [11]. This paper was restricted to the case of 3D linear filaments without a phase twist. One of the important properties of the three-dimensional spiral waves of the CGLE is the possibility of scroll waves with a phase twist along the filament direction, which we refer to as a ''phase-twisted filament.'' It was shown in [9] that straight filaments with a small twist were stable at long wavelength, but the stability at shorter wavelength was not examined. In addition, we have recently received a preprint [12] in which the authors study the evolution of phase-twisted filaments using a three-dimensional nonlinear code. In this paper we investigate the stability of a straight filament with arbitrary phase twist. For this purpose, we use a linearized set of equations for perturbations to the phase-twisted straight filament. Stability diagrams in the (α,β) parameter space obtained from the linear stability code are presented and discussed. Using a full three-dimensional nonlinear simulation, evolution to nonlinear states in the form of helical filaments is observed for cases we tested near the boundary of the unstable region of the phase-twisted straight filament.

II. PERTURBATION EQUATION

A. Spiral wave solution of 2D CGLE

The spiral wave solution of the two-dimensional CGLE has the form

$$A_0(r,\theta,t) = \rho(r)\exp\{i[-\omega t + \sigma\theta + \psi(r)]\}, \tag{2}$$

where $\sigma = \pm 1$ is the ''topological charge,'' (r,θ) are polar coordinates (later, z direction will be added for the consideration of the three-dimensional spiral wave), and $\rho(r)$ and $\psi(r)$ are real. The phase change of A_0 going counterclockwise around the origin is $2\pi\sigma$. The amplitude of A_0 at the origin is zero due to the phase singularity there. Thus the spiral wave can be viewed as a vortex whose center is a

*Author to whom correspondence should be addressed. FAX: 301-405-1678. Electronic address: kynam@chaos.umd.edu

†Also at Department of Physics, Department of Electrical Engineering, and Institute for Systems Research, University of Maryland, College Park, Maryland 20742.

‡Present address: Laboratory of Applied Mathematics, Mt. Sinai School of Medicine, One Gustave L. Levy Place, New York, NY 10029-6574.

topological point defect. For large distances from the defect, the wave front asymptotically approaches a plane wave with a wave number k. Thus as $r\to\infty$,

$$\rho\to\sqrt{1-k^2},\quad \frac{d\psi}{dr}\to k, \tag{3}$$

where k is uniquely determined by the parameters α and β [3,13]. The frequency of the spiral is given by the plane wave dispersion relation, $\omega=\alpha+(\beta-\alpha)k^2$. As $r\to 0$

$$\rho\to 0,\quad \frac{d\psi}{dr}\to 0. \tag{4}$$

Note that the sign of k has to be chosen so that the radial group velocity is outgoing, $v_g=2(\beta-\alpha)k>0$ or $\mathrm{sgn}(k)=\mathrm{sgn}(\beta-\alpha)$. Inserting Eq. (2) into Eq. (1) yields a nonlinear eigenvalue equation for $\rho(r)$ and $\psi(r)$ which can be numerically solved [3] for $k(\alpha,\beta)$ with the boundary conditions (3) and (4). (In our work we solved this problem using the relaxation method [14].)

A solution representing a filament with constant phase twist κ can be constructed by writing $A_1=a_1(r)\exp i(-\omega_1 t+\sigma\theta+\kappa z)$. Inserting this ansatz into the CGLE (1), one can obtain [9] the following relationships between the solution for a filament with no twist (subscript 0) and one with twist (subscript 1):

$$\omega_1=\omega_0+(\beta-\omega_0)\kappa^2, \tag{5}$$

$$a_1(r)=\sqrt{1-\kappa^2}\,a_0(\hat{r}), \tag{6}$$

where $a_0=\rho_0(r)e^{i\psi_0(r)}$ and ω_0 are the radial direction dependence and the frequency of the spiral solution of two-dimenstional CGLE, repectively, and $\hat{r}$ is a scaled radial coordinate, $\hat{r}=r\sqrt{1-\kappa^2}$. Thus the solution for a three-dimensional straight filament with twist can be constructed from the two-dimensional solution by rescaling the frequency, amplitude, and radial variable. The radial asymptotic wave number of a spiral wave solution with phase twist, k_1, becomes $k_0\sqrt{1-\kappa^2}$, where k_0 is the asymptotic wave number for the two-dimensional spiral wave solution (filament with no twist) and the total large r asymptotic wave vector is given by

$$\vec{k}_t=\kappa\hat{z}+k_1\hat{r}, \tag{7}$$

$$k_t=\sqrt{{k_0}^2+(1-{k_0}^2)\kappa^2}. \tag{8}$$

B. Perturbation equations for a straight filament with twist

We assume that the equilibrium and perturbed solution has the form

$$A(r,\theta,s,t)=[a_1+u(r,\theta,z,t)]\exp\{-i\omega_1 t+i\sigma\theta+i\kappa z\}, \tag{9}$$

where u is the linear perturbation imposed on a_1, the equilibrium solution derived in the preceding section. Substituting Eq. (9) into the CGLE (1) and assuming $u(r,\theta,z,t)=u_+e^{st+ik_z z+im\theta}+\overline{u_-}e^{s^*t-ik_z z-im\theta}$, we obtain the following linearized system of equations for u_+ and u_-:

$$(-i\omega_1+s)u_+=u_++(1+i\beta)\times\left(\frac{1}{r}\frac{\partial}{\partial r}r\frac{\partial}{\partial r}-\frac{(m+\sigma)^2}{r^2}-(k_z+\kappa)^2\right)u_+ -2(1+i\alpha)|a_1|^2u_+-(1+i\alpha)a_1^2u_-, \tag{10}$$

$$(i\omega_1+s)u_-=u_-+(1-i\beta)\times\left(\frac{1}{r}\frac{\partial}{\partial r}r\frac{\partial}{\partial r}-\frac{(m-\sigma)^2}{r^2}-(k_z-\kappa)^2\right)u_- -2(1-i\alpha)|a_1|^2u_--(1-i\alpha)\overline{a_1^2}u_+. \tag{11}$$

We will consider $m=1$ in this paper. Dividing by $1-\kappa^2$ and defining a new radial coordinate $\hat{r}=r\sqrt{1-\kappa^2}$, a scaled wave number $\hat{k}_z=k_z/\sqrt{1-\kappa^2}$, a scaled twist $\hat{\kappa}=\kappa/\sqrt{1-\kappa^2}$, and a scaled growth rate $\hat{s}=s/(1-\kappa^2)$ we obtain

$$\left[i\omega_0-\hat{s}+1+(1+i\beta)\times\left(\frac{1}{\hat{r}}\frac{\partial}{\partial\hat{r}}\hat{r}\frac{\partial}{\partial\hat{r}}-\frac{(m+\sigma)^2}{\hat{r}^2}-(\hat{k}_z{}^2+2\hat{k}_z\hat{\kappa})\right) -2(1+i\alpha)|a_0|^2\right]u_+-(1+i\alpha)a_0^2u_-=0, \tag{12}$$

$$\left[-i\omega_0-\hat{s}+1+(1-i\beta)\times\left(\frac{1}{\hat{r}}\frac{\partial}{\partial\hat{r}}\hat{r}\frac{\partial}{\partial\hat{r}}-\frac{(m-\sigma)^2}{\hat{r}^2}-(\hat{k}_z{}^2-2\hat{k}_z\hat{\kappa})\right) -2(1-i\alpha)|a_0|^2\right]u_--(1-i\alpha)\overline{a_0^2}u_+=0, \tag{13}$$

where we use Eq. (5) and the relationship between a_1 and a_0, $a_0(\hat{r})=a_1(r)/\sqrt{1-\kappa^2}$. In this form, the numerical solution for a radially dependent function (i.e., a_0) from the 2D CGLE is explicitly independent of the twist κ, and, after the trivial rescalings of s and k_z, the twist parameter $\hat{\kappa}$ appears only in the terms $\pm 2\hat{k}_z\hat{\kappa}$. (See Sec. III A for boundary conditions.) For small k_z and κ, Eqs. (12) and (13) can be analytically solved using the technique in [9]. To lowest order in $k_z\sim\kappa^2$, we obtain damping of a straight filament perturbation,

$$s=-(1+\beta^2)k_z^2. \tag{14}$$

Another solvable case occurs for κ^2 close to, but less than, one (recall that we require $1-\kappa^2>1$ for existence of the twisted equilibrium, Sec. II A). In this case, to lowest order in $(1-\kappa^2)$ Eqs. (12) and (13) reduce to $[s+(1\pm i\beta)({k_z}^2\pm 2k_z\kappa)]u_\pm\cong 0$, which yields the solutions s

$\cong -(1+i\beta)(2k_z\kappa+k_z^2)$ (with $|u_+| \gg |u_-|$) and $s \cong (1-i\beta)(2k_z\kappa-k_z^2)$ (with $|u_-| \gg |u_+|$). In both cases there is instability (either for $0>k_z>-2\kappa$ or $0<k_z<2\kappa$). This simple case clearly shows the potential destabilizing effect of twist.

III. NUMERICAL STABILITY RESULTS

A. Numerical methods

In order to find the growth rate Re(s) numerically, we use the following scheme. If we replace s with the partial time derivative $\partial/\partial t$ operator, Eqs. (12) and (13) become time-dependent partial differential equations in one spatial variable, $\hat{r}$. We solve these coupled linear equations using a semi-implicit split-step method. The typical number of mesh points used in our studies is 400, but for certain parameter values of α, β, we increased the resolution to 1000, or 2000 mesh points for the purpose of double checking the results. The maximum length of the radial box size used ranges from 20 to 40 (for some cases, 70 or 100). The behavior of u_+ and u_- as r goes to zero, is

$$u_+(r) \to r^2, \qquad u_-(r) \to \text{const} + O(r^2). \tag{15}$$

Thus, at $r=0$, we use the boundary conditions that $u_+(0)=0$ and $du_-/dr|_0=0$. For the boundary condition at large r, we use $u_+(L_{\max})=u_-(L_{\max})=0$. As noted earlier, the defect launches outgoing waves. Furthermore, we are interested in the (α,β) regime where these outward plane waves are not absolutely unstable (Sec. V). In this case inward waves excited at $r=L_{\max}$ are rapidly damped and our condition at $r=L_{\max}$ serves as an effective absorbing boundary for outgoing waves. For the purpose of examining the sensitivity of the eigenvalues and eigenfunctions to the boundary conditions at large r, we have varied $L_{\max}$ for several parameters and found no significant (less than 0.1%) differences in the computed growth rate. By taking a random initial condition or a Gaussian-like initial condition (which we have chosen in this paper), the numerical solution relaxes to the eigenmode which has the largest growth rate. We record the growth at each instant of time and use a stringent convergence criterion to accept the computed value as a legitimate growth rate. To validate the code, we first considered the case for small k_z and $\kappa=0$, a region of parameter space where Eq. (14) applies. Figure 1 shows that the numerical result (open circles) closely follows the theoretical damping rate (solid curve) (14) for $\alpha=0.6$, $\beta=-0.5$. We also have tested other parameter values. Due to small numerical error, the numerically computed magnitude of the growth rate for $k_z=0$ is typically of the order of 10^{-4} (rather than the theoretical result of zero).

B. Parameter space for filament stability

We first address the stability of a filament with no twist and compare our results with those previously obtained by Aranson *et al.* [15] using a different numerical method. In Fig. 2(a), the phase diagram of the straight filament without phase twist is presented. In the region to the right of the circles, the straight filament is unstable to the perturbation

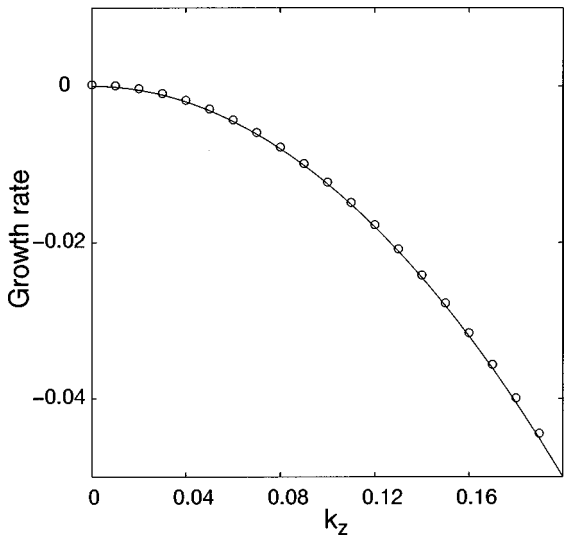

FIG. 1. Comparison between the numerical results and theoretical results for small k_z with $\alpha=0.6$, $\beta=-0.5$. Circles correspond to the numerical results and the solid line is from the theoretical results, $s=-(1+\beta^2)k_z^2$, where s is growth rate, k_z is the wave number of modulation along the straight filament.

with a finite k_z. These results are consistent with the work of Aranson *et al.* [15] for the straight filament with no twist. Above the solid line, the asymptotic plane wave of the spiral wave becomes absolutely unstable. For the phase-twisted straight filament the stability boundary in α, β parameter space is shown in Figs. 2(b), 2(c), and 2(d) for phase-twist wave number $\kappa=0.1$, 0.15, and 0.2, respectively. The circles (dots) represent parameter values numerically found to be unstable (stable). Compared to the case of the untwisted filament, it is seen that the stable region of parameters is reduced by twist. It is also observed that an additional unstable region emerges for low values of $-\beta$ [e.g., the circles in $-\beta<1$ for Fig. 2(c)], which does not exist for the untwisted case. As the phase twist increases, the stable region of the straight filament gets smaller.

In Fig. 3 the growth rate versus k_z is shown for $\alpha=0.1$, $\beta=-1.0$, and $\kappa=0.15$. These values correspond approximately to a marginally stable situation [see Fig. 2(c)]. We note that for $k_z<0.1$ the growth rate is negative and in approximate conformity with the theoretical result (14). Near $k_z \sim 0.1$ there appears to be a mode crossing in the sense that an eigenfunction that is more strongly damped for $k_z<0.1$ than the eigenfunction corresponding to Eq. (14) becomes less strongly damped for $k_z \gtrsim 0.1$. As k_z is increased past 0.1 the growth rate of this eigenfunction rises, becoming maximum at $k_z=k_z^{\max}=0.2$. At this maximum the growth rate is near zero. For the same α and κ values, the growth rate at $k_z^{\max}$ increases (becomes positive corresponding to instability) as $-\beta$ increases from its marginal stability value, and it decreases (becomes negative, corresponding to stability) when $-\beta$ is decreased from its marginal stability value. (Note from Fig. 3 that $k_z^{\max} \neq \kappa$.) The same mode crossing phenomenon observed for $\kappa=0.15$ (Fig. 3) is also found for other values of κ including the untwisted case ($\kappa=0$). Hence we see that, although the long wavelength analysis yielding the result (14) continues to hold in the unstable regime, the stable long wavelength modes will eventually be

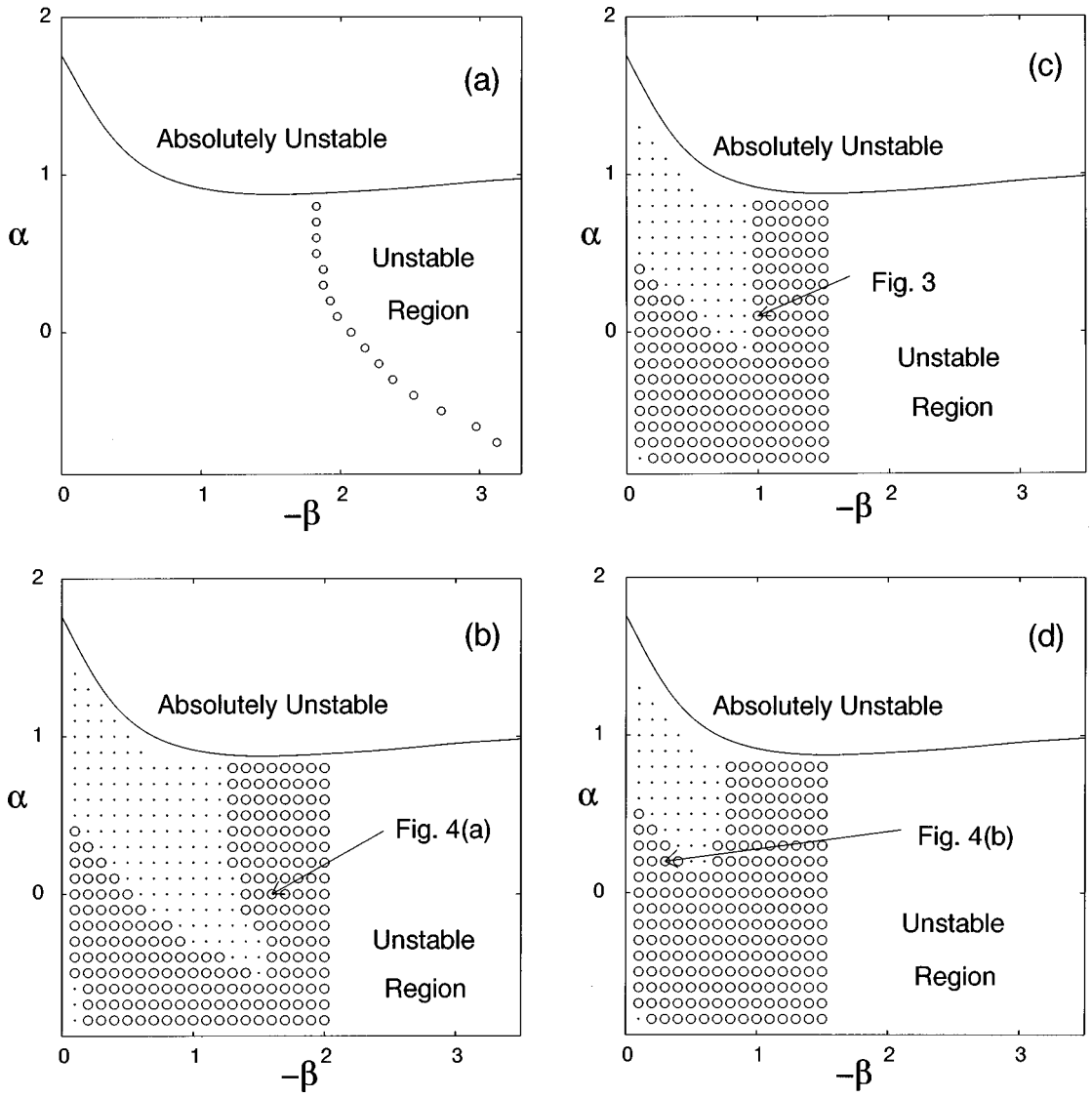

FIG. 2. Phase diagrams with various values of the phase twist. (a) $\kappa=0.0$ case (untwisted). To the right of the circles, the straight filament is unstable. At the region of the parameters above the solid line, the spiral wave is absolutely unstable. (b) Phase diagram for $\kappa=0.1$, in the region with circle and the region to the right of the circled region, the straight filament with the phase twist $\kappa=0.1$ is unstable. (c) Phase diagram for $\kappa=0.15$. Same as (b) with $\kappa=0.15$. The region where the filament is stable is smaller than the case of (b). (d) Phase diagram for $\kappa=0.2$. Same as (b) with $\kappa=0.2$.

overcome by short wavelength unstable modes not described by the long wavelength perturbation analysis that gives Eq. (14). Thus the results of Ref. [9] yielding the slow evolution of arbitrarily shaped filaments with weak curvature (analogous to long wavelength) and weak phase twist are physically relevant only in the regime where the filament is stable to short wavelength modes. We emphasize, however, that the stable region where the results of Ref. [9] are physically relevant is relatively large, particularly for small or zero twist.

IV. THREE-DIMENSIONAL NONLINEAR SIMULATION RESULTS

The full numerical simulation of the three-dimensional CGLE has been done using periodic boundary condition in x, y, and z via a time split-step technique. In the first step, the nonspatial part of the CGLE $\partial A/\partial t=A-(1+i\alpha)|A|^2A$ is solved exactly by $A(t+\Delta t)=A(t)e^{\Delta t}[1+|A(t)|^2(e^{2\Delta t}-1)]^{-(1+i\alpha)/2}$. Then, in the second step, the diffusive part, $\partial A/\partial t=(1+i\beta)\nabla^2A$, is solved by fast Fourier transforming to the wave number space $[A(\vec{x},t)\rightarrow\tilde{A}(\vec{k},t)]$, integrating analytically $(\tilde{A}(t+\Delta t)=\tilde{A}\exp[-(1+i\beta)k^2\Delta t])$, and transforming back to real space $(\tilde{A}\rightarrow A)$.

The straight vortex filament is used as an initial condition for the three-dimensional simulation. For topological reasons, there are always two of them with opposite charge in the box. To ensure that the interaction between the pair and interactions with vortices in other periodicity cells do not significantly influence the instability, we used a large computational box. Theory predicts that vortex interaction is exponentially small in the distance between vortices. The assumed lack of significant vortex interaction is supported by the observation that during the linear phase of the growth of the instability, the growth rates obtained from the 3D code were in reasonable agreement with results from our single filament vortex linear stability code.

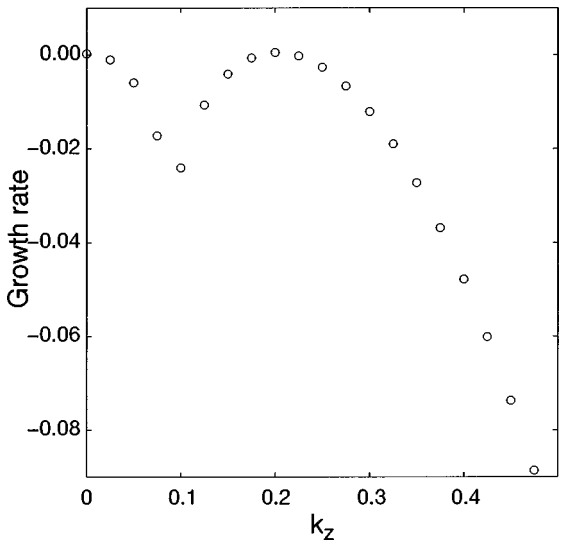

FIG. 3. The growth rate versus k_z with $\alpha=0.1$, $\beta=-1.0$, $\kappa=0.15$, when the parameters are on the boundary of the unstable region. Note that the $k_z^{\max}$ which gives the instability at finite k_z has different value from the wave number of the phase twist, $\kappa=0.15$.

Figure 4(a) shows a final helical state resulting from saturation of such an instability for the case $\alpha=0.0$, $\beta=-1.6$ with the phase twist $\kappa=0.1$. These parameters are just to the right of the stability boundary [see Fig. 2(b)]. The pitch of the helix has a value of $2\pi n/L_z$ with the integer n equal to 4. This corresponds to $k_z^{\max}$ calculated from our linear stability analysis. Another interesting unstable region of the straight filament with the nonzero phase twist is where the parameter $-\beta$ is smaller. In this region, the linear stability analysis shows a very weak instability (usually the growth rate is less than 10^{-2}). Figure 4(b) shows a helical structure evolved from an unstable initially straight filament for $\alpha=0.2$, $\beta=-0.3$, $\kappa=0.2$ [see Fig. 2(d)]. For this case (the box size $L_x=50\pi$, $L_y=50\pi$, $L_z=20\pi$) the helical structure keeps growing. Eventually parts of the two helices of opposite charge approach each other and reconnect [16]. (We cannot rule out the possibility that with a bigger box size, a saturated helical state might result.)

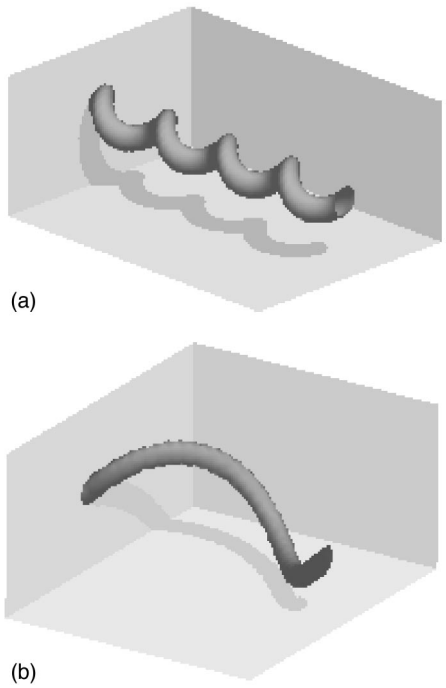

FIG. 4. (a) Helical vortex filament for $\alpha=0.0$, $\beta=-1.6$ with the phase twist $\kappa=0.1$. $L_x=20\pi$, $L_y=20\pi$, $L_z=40\pi$, mesh size$=64^3$. Isosurface $|A|=0.65$ is shown. (b) Helical vortex filament for $\alpha=0.2$, $\beta=-0.3$ with the phase twist $\kappa=0.2$. $L_x=50\pi$, $L_y=50\pi$, $L_z=20\pi$, mesh size equal to $128\times128\times32$. Isosurface $|A|=0.85$ is shown.

V. ABSOLUTE INSTABILITY OF THE ASYMPTOTIC PLANE WAVE OF A TWISTED FILAMENT

We now investigate the change in the absolute stability boundary for a filament with phase twist. We find that this change is rather small for the κ values we investigate. As discussed in Sec. II A, a filament with phase twist has a large r asymptotic wave number different from that of the untwisted filament. This causes a change of the condition for the absolute instability of the asymptotic plane wave solution.

The complex growth rate $\lambda(\vec{q})$ for a modulational perturbation to the plane wave solution with spatial dependence $e^{\pm i\vec{q}\cdot\vec{x}}$ is

$$\lambda(\vec{q})=-q^2-2i\beta\vec{k}_t\cdot\vec{q}-R_{k_t}^2 \pm\sqrt{(1+\alpha^2)R_{k_t}^4-(\beta q^2-2i\vec{k}_t\cdot\vec{q}+\alpha R_{k_t}^2)^2}, \quad (16)$$

where $R_{k_t}^2=1-k_t^2$. The above equation has the same form as the growth rate for the two-dimensional spiral wave case, with k_0 replaced by $k_t=\sqrt{\kappa^2+(1-\kappa^2)k_0^2}$. The time evolution of the perturbation, $u(x,t)$, is given by

$$u(\vec{x},t)=\int_{-\infty}^{+\infty}d^3\vec{q}\,\exp[i\vec{q}\cdot\vec{x}+\lambda(\vec{q})t]u_{\vec{q}}(t=0), \quad (17)$$

where $u_{\vec{q}}(t=0)$ is the Fourier transform of an initial perturbation which is three-dimensionally localized about some point $\vec{x}_0$. For $t\to\infty$, this integral can be evaluated at the point $\vec{x}_0$ using the saddle point method. Then the condition for absolute instability becomes [5,17]

$$\mathrm{Re}[\lambda(\vec{q}^*)]>0, \quad (18)$$

$$\left(\frac{\partial\lambda(\vec{q})}{\partial\vec{q}}\right)_{\vec{q}^*}=0, \quad (19)$$

$$\left[\mathrm{Re}\left(\frac{\partial^2\lambda(\vec{q})}{\partial\vec{q}\,\partial\vec{q}}\right)\right]_{\vec{q}^*}<0, \quad (20)$$

where the third of these conditions indicates that the real part of the matrix of partial derivatives $\partial^2\lambda/\partial\vec{q}\,\partial\vec{q}$ is negative definite. It is convenient to use $\vec{q}$ coordinates $\vec{q}=q_\parallel(\vec{k}_t/|\vec{k}_t|)+\vec{q}_\perp$ with $\vec{q}_\perp\cdot\vec{k}_t\equiv0$. From Eq. (16) we see that λ depends on $\vec{q}_\perp$ only through $q_\perp^2$ and hence $\partial\lambda/\partial\vec{q}_\perp=0$ for $\vec{q}_\perp=0$. Thus we take $\vec{q}$ to be parallel to $\vec{k}_t$ and Eqs. (19) and

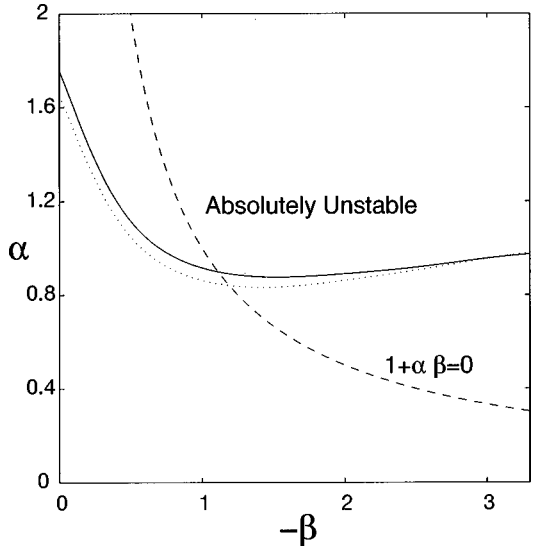

FIG. 5. Diagram showing the absolute instability line. The solid line is for the untwisted case, and the dotted line is for the case of the phase-twisted case with $\kappa=0.2$. The dashed line is for the Benjamin-Feir instability, $1+\alpha\beta=0$, where all the plane wave solutions are unstable.

(20) become $\lambda(q_\parallel^*,\vec{q}_\perp=0)>0$, $[\partial\lambda(q_\parallel,\vec{q}_\perp=0)/\partial q_\parallel]_{q_\parallel=q_\parallel^*}=0$. From these conditions, we compute a marginal stability line in (α,β) space. To check that Eq. (20) is satisfied along this line we note that the matrix $\partial^2\lambda(\vec{q})/\partial\vec{q}\partial\vec{q}$ is diagonal at $\vec{q}_\perp=0$, and thus Eq. (20) becomes the two scalar conditions $\mathrm{Re}[\partial^2\lambda/\partial q_\parallel^2]<0$, $\mathrm{Re}[\partial^2\lambda/\partial q_\perp^2]<0$ at $q_\parallel=q_\parallel^*$, $\vec{q}_\perp=0$. We find these to be satisfied on the computed marginal stability line. The solid line in Fig. 5 is the stability curve for the asymptotic plane wave of the untwisted filament and the dotted line is for the result for a phase-twist wave number of $\kappa=0.2$. As can be seen, a phase-twisted filament becomes absolutely unstable for smaller values of α (for $\beta>-2.8$) compared to an untwisted filament. For $\beta<-2.8$, one can see the crossing of the two stability lines. However, in this parameter region, the phase-twisted filament is already unstable due to the instability discussed earlier.

VI. CONCLUSION

A time-dependent code, using a split-step algorithm, was developed to investigate the linear stability of twisted CGLE filaments. The code was benchmarked by comparing results with analytical solutions of Gabbay *et al.* [9] for the small k_z case. The agreement was excellent. For the filament with no twist, the stability boundary for the core instability was determined in the (α,β) parameter space. This boundary was found to be in good agreement with the recent work of Aranson *et al.* [15] who use a different numerical technique. We then studied the stability boundary for scroll wave filaments with twist. It was found that the twist reduces the stable region of the straight linear filament. Nonlinear saturated or growing helical states that develop due to the instability have been obtained using our three-dimensional nonlinear code [9]. The stable region of the straight filament in parameter space shrinks as the phase-twist wave number is increased. The absolute instability analysis for the asymptotic plane wave solution of a three-dimensional spiral wave with phase twist shows that there is a shift of the stability boundary. This shift in the absolute plane wave stability boundary is small even with a phase twist large enough to significantly reduce the stability region (e.g., $\kappa=0.2$).

ACKNOWLEDGMENT

This work was supported by the U.S. Office of Naval Research (Physics).

[1] For a general review on pattern formation see M. C. Cross and P. C. Hohenberg, Rev. Mod. Phys. **65**, 851 (1993).
[2] Y. Kuramoto, *Chemical Oscillations, Waves and Turbulence* (Springer, Berlin, 1984).
[3] P. S. Hagan, SIAM (Soc. Ind. Appl. Math.) J. Appl. Math. **42**, 762 (1982).
[4] T. Bohr, G. Huber, and E. Ott, Europhys. Lett. **33**, 589 (1996); Physica D **106**, 95 (1997).
[5] I. S. Aranson, L. Aranson, L. Kramer, and A. Weber, Phys. Rev. A **46**, R2992 (1992).
[6] G. Huber, P. Alstrom, and T. Bohr, Phys. Rev. Lett. **69**, 2380 (1992).
[7] H. Chate and P. Manneville, Physica A **224**, 348 (1996).
[8] P. Coullet, L. Gil, and J. Lega, Phys. Rev. Lett. **62**, 1619 (1989).
[9] M. Gabbay, E. Ott, and P. Guzdar, Phys. Rev. Lett. **78**, 2012 (1997); Physica D (to be published).
[10] I. S. Aranson, and A. R. Bishop, Phys. Rev. Lett. **79**, 4174 (1997).
[11] I. S. Aranson, L. Kramer, and A. Weber, Phys. Rev. Lett. **72**, 2316 (1994).
[12] G. Rousseau, H. Chate, and R. Kapral, Phys. Rev. Lett. **80**, 5671 (1998). We received a copy of this work while completing our present paper. This work is complementary to ours in that it extensively investigated the nonlinear state but does not examine stability using a linear code. Another main result Rousseau *et al.* found is the existence of ''supercoiled'' nonlinear states when the phase twist exceeds a certain critical value.
[13] E. Bodenschatz, A. Weber, and L. Kramer, in *Nonlinear Processes in Excitable Media*, edited by A. V. Holden, M. Markus, and H. G. Othmer (Plenum, New York, 1990).
[14] W. H. Press, B. P. Flannery, S. A. Teukolsky, and W. T. Vetterling, *Numerical Recipes* (Cambridge University Press, Cambridge, England, 1986).
[15] I. Aranson, A. R. Bishop, and L. Kramer, Phys. Rev. E **57**, 5276 (1998).
[16] M. Gabbay, E. Ott, and P. Guzdar (unpublished).
[17] L. D. Landau and E. M. Lifshitz, *Fluid Mechanics* (Pergamon, London, 1959).